

Middle-lower continental crust exhumed at the distal edges of volcanic passive margins

Laurent Geoffroy ¹✉, François Chauvet¹ & Jean-Claude Ringenbach²

The extent of continents in oceans is an important scientific, economic and political issue. The crustal types seaward of the necking zones of volcanic passive margins are investigated. From a set of high-quality seismic data from Namibia we discuss the nature of this crust, oceanic or continental. Here we show that over ~100 km, this crust shares few of the characteristics of oceanic crust born from accretion at a slow-spreading oceanic ridge. We alternatively suggest that the middle-lower continental crust could be exhumed and made brittle at the most distal end of volcanic passive margins. We consecutively distinguish the mechanical break-up of the continental lithosphere at volcanic passive margins, i.e., the drop in mechanical strength, from a stage of steady-state syn-magmatic extension, most probably subaerial, predating the onset of the purely magmatic oceanic crust. These findings suggest that the extent of continental material in oceans could be more significant than isolated continental blocks and microcontinents.

¹Geo-Ocean, CNRS, IFREMER, Université de Bretagne Occidentale, Brest, France. ²TOTAL SA, Pau, France. ✉email: laurent.geoffroy@univ-brest.fr

Passive margins are formed from successful continental rifting, involving mechanical extension. At volcanic passive margins (VPMs), continental extension is distinctly coeval with abundant mafic magmatism above a continuously melting asthenosphere^{1,2}. At both VPMs³ (Fig. 1A) and non-VPMs⁴ (Fig. 1B), a crustal necking zone generally divides two distinct domains, proximal and distal (Fig. 1). This necking zone is characterized by a steeply dipping Moho associated with a strong gradient in crust thinning and stretching (Fig. 1). At VPMs, the proximal and necking domains are specifically associated with inner SDRs (seaward-dipping reflectors). Inner SDRs consist of thick wedges of compound or/and thick lava flows emplaced subaerially^{5–7}, intruded by sills and dykes^{6–8} with no or anecdotal interlayered sediments^{5–7} except, locally, at their very top⁹. Purely isostatic analytical models for SDRs development¹⁰ fail to account for direct observations of SDR growth¹¹ and structure^{3,7,8}. Inner SDRs are bounded by continentward-dipping listric normal faults that flatten at the top of a ductile middle or lower crust^{5,7,9,12,13} (Fig. 1A).

To seaward of the necking zone, in the distal (or outer) domain, the exhumed continental mantle is frequently documented at non-VPMs⁴ (Fig. 1B). The boundary between continental and oceanic lithosphere is usually very abrupt and marked by a positive basement step (Fig. 1B). The distal domain of VPMs is very different and poorly explored (Fig. 1A). It generally shows a crust with a clearly defined Moho (Figs. 2 and 3). In its upper part, it is characterized by outer SDRs and/or by the so-called “flat-lying (volcanic) flows” (herein FLFs)^{9,14,15}. Outer SDRs are generally shorter in length and more arcuate at their distal seaward end than are inner SDRs^{3,9}. Their extremities appear to lean against flat-lying subhorizontal surfaces, top of a crust of unknown composition (Figs. 3 and 4)^{9,14–16}. The FLF-bearing upper crust is still more poorly defined^{14–16}. It is unclear

to date if FLFs are, or not, a distinct type of outer SDRs^{9,16}. This crust type may occur continentward regarding the outer-SDR type, or not (this paper). FLF-bearing upper crust is associated with bright and horizontal reflections to its top, interpreted as lavas¹⁵. Below is a poorly defined medium with some low-angle seaward-dipping reflectors^{14–16}. A remarkable set of bright reflections, the UCR^{15,16} (upper crustal reflections) lies 0.5–1.5 s of TWT beneath the acoustic basement.

Because outer SDRs generate clear linear magnetic anomalies (Supplementary Fig. 1)^{17,18}, the outer domain at VPMs is often considered as made up of oceanic-type lithosphere, e.g.,¹⁷. However, a continuity of the continental lower crust from inner- to outer VPMs has recently been suggested based on seismic refraction¹⁹ and seismic reflection surveys²⁰. Nevertheless, the supporting seismic reflection data were of limited depth extent and/or of medium quality. We recently reviewed the extensive set of depth-converted seismic reflection lines of high quality from IONTM in the South Atlantic⁸. Here, we focus our analysis on the most distal edges of the Namibian VPMs mostly using the NamibiaSPANTM dataset from IONTM (Fig. 2). We perform new observations of the distal domain of these VPMs. We discuss the continental or oceanic nature of the crust types based on a review of the distinctive features of the oceanic crust generated at slow-spreading ridges. We argue that the abrupt assertion of the oceanic-crust nature of the distal VPMs in Namibia and elsewhere is not scientifically established and that a continental interpretation is possible.

Results

Moho topology and seismic facies at distal Namibia VPMs. The necking zone at the distal edges of Namibia-Span lines presents a Moho slope varying between 7.4° and 14.7° (Figs. 2 and 3). A key and systematic feature is the presence of narrow crustal thin points seaward of the necking zone (Fig. 2). Crustal thin points are defined by a thinner crust regarding the crust located seaward, herein named the distal crustal bulge (Figs. 2 and 3). The distal crustal bulge is wide (~100 km) and characterized by a crust swelled in its lower part. The crustal thickness ratio between the distal crustal bulge and the crustal thin point is constant (1.36 ± 0.16), whatever the distal crustal bulge thickness. The distal crustal bulge area corresponds to the outer SDRs or/and FLF crust types (Figs. 2 to 4). It ends seaward when crust thickness is constant (red arrows in Fig. 2). A similar pattern is found in the conjugate margins of S America⁸.

Inner-SDR crust (necking zone). A common observation in Namibia (and elsewhere⁹), is the capping of the seaward-most inner-SDR wedge by a large planoconvex or lenticular structure dipping seaward (Supplementary Fig. 6a, b). The upper continental crust beneath the inner SDR wedges is relatively transparent. A more reflective and thickened middle/lower crust underlies the upper crust, with two distinct seismic facies⁸ (named LC1 and LC2 in ref. ¹³) (Figs. 3 and 4). At the necking zone, LC1 P-waves present both high velocities ($\sim 7.2\text{--}7.3 \text{ km.s}^{-1}$ in average) and small gradients with depth²¹ (Supplementary Fig. 2 and 3). LC1 shows a system of bright and thick oblique reflectors dipping seaward, which are planar, curved as sigmoid flexures¹² or even “folded”¹³. Along the Moho slope, these reflectors are curved along the LC2 facies where they merge (Figs. 3 and 4e–f). LC2 is highly reflective, typically 4–5-km thick, with layering subparallel to the Moho. It is associated with the strongest P-wave velocities ($\sim 7.6 \text{ km.s}^{-1}$, Fig. 3b)²¹. The LC2 facies continues beneath both the crustal thin point and the distal crustal bulge (Figs. 3 and 4, Supplementary Fig. 4).

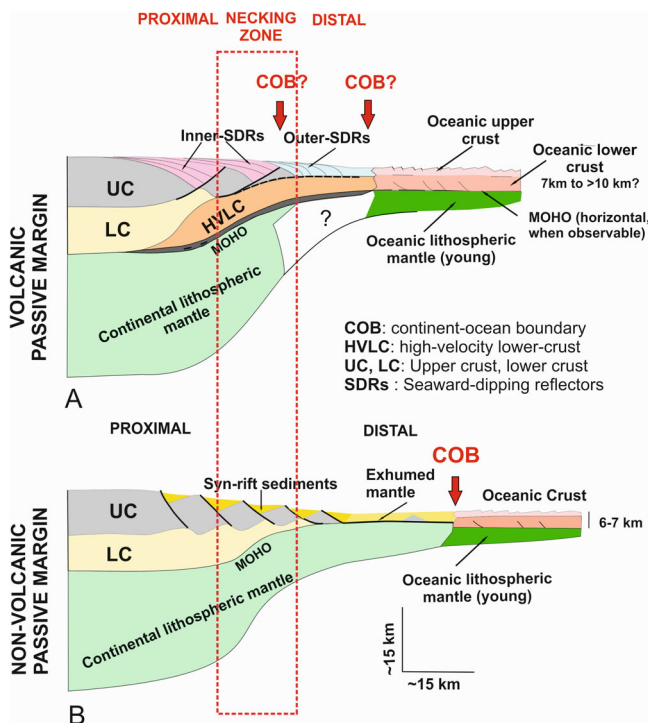


Fig. 1 Simplified sketches of crustal domains at passive margins.

A Volcanic passive margins. Based from the present study and from a synthesis of crustal-scale observations at VPMs^{1–3,8,12,13,18,21,22,41,43,45,48–50}; **B** nonvolcanic passive margins simplified from^{51,52}.

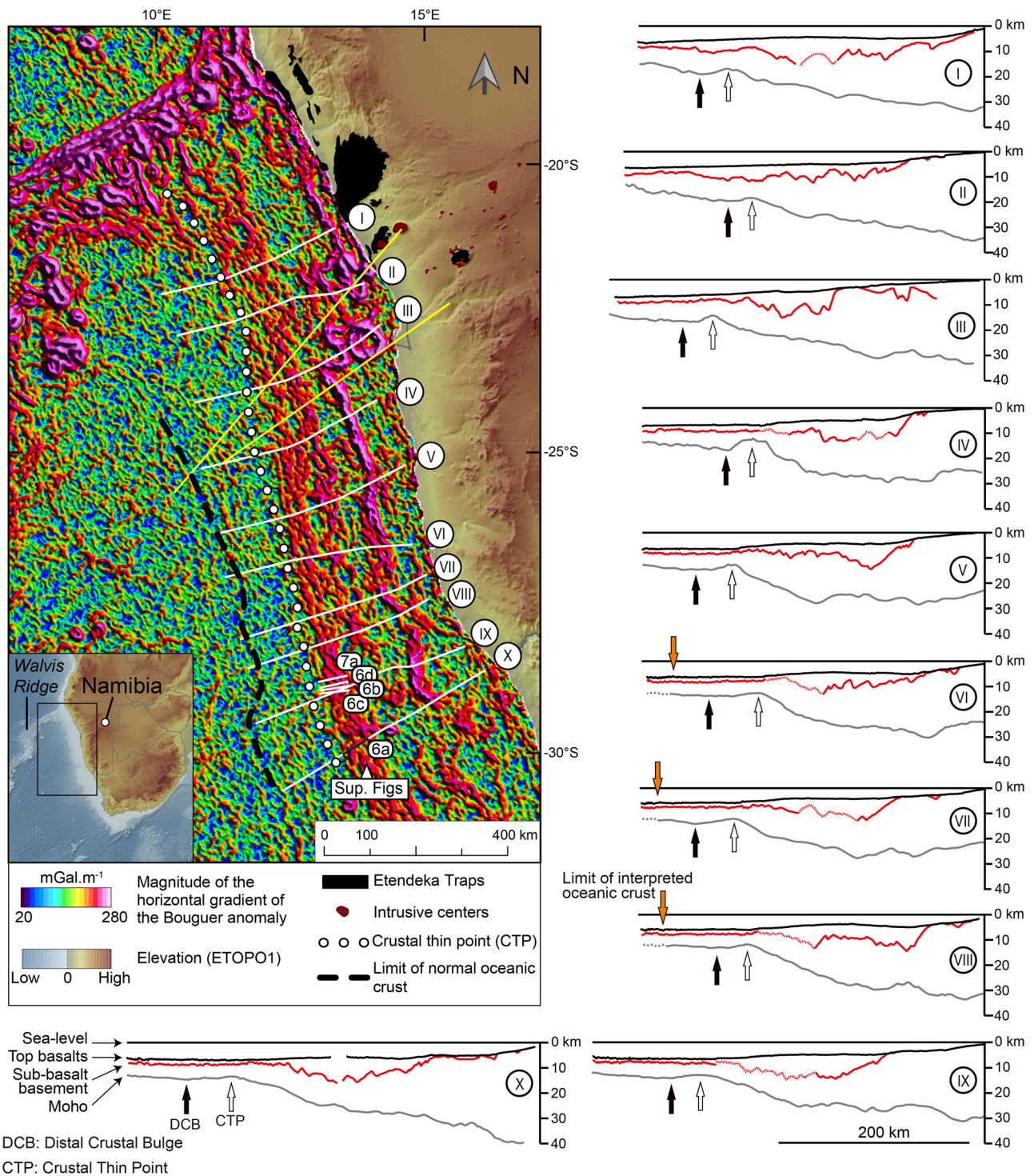


Fig. 2 Location of the seismic lines on a gravity map and crustal-scale line drawing. Left: horizontal gradient magnitude of the Bouguer anomaly along the Namibia margins. Magnetic anomalies in Supplementary Fig. 1. Numbers I–X refer to the seismic lines that we used (NamibiaSPAN™ from ION™). Information about the depth conversion of time lines is found in Supplementary Figs. 2 and 3. Yellow: seismic refraction lines²¹. Right and bottom: simplified line drawings from depth-converted lines.

Outer-SDR crust. The outer-SDR crust type is common along the S-America VPMs^{8,9,14} which is not the case in offshore Namibia. We observe that outer-SDR wedges grow seaward mimicking prograding and slightly aggrading foresets as observed in sedimentary basins (Fig. 4c; Supplementary Figs. 5c and 6a). Outer SDRs may also be associated with distinct (albeit discrete) subsets of

edge reflectors tapping onto low-dipping continentward dipping discontinuities located top of a transparent crust unit (Fig. 4c; Supplementary Fig. 5c). Significantly, no clear lateral variations in seismic facies and seismic velocity ($V_p \sim 7.2\text{--}7.3 \text{ km.s}^{-1}$) are observed from the necking zone LC1 to the outer-SDR lower crust^{13,21} (Figs. 3b and 5 and Supplementary Figs. 2 and 3).

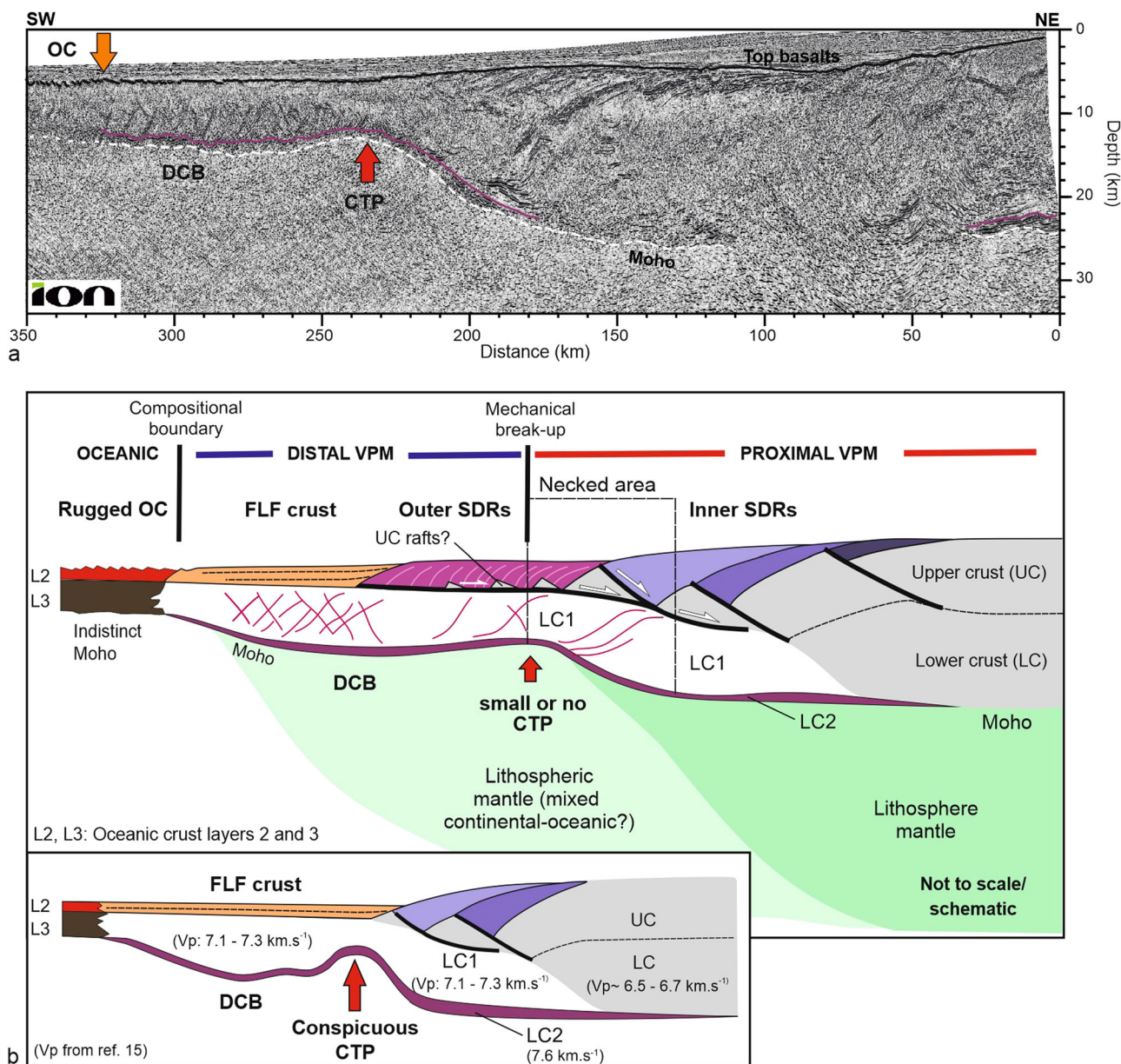


Fig. 3 Crustal structure of VPMs offshore Namibia. **a** Selected line with crustal thin point (CTP) and distal crustal bulge (DCB) (IONTM line VI, Fig. 2). **b** Synthetic VPM models from the studied seismic lines. Main drawing: VPM with outer-SDR and FLF crust types (lines II and III, Fig. 2). Infra: with FLF crust only (lines I and IV-X, Fig. 2). Full seismic velocities can be found in Supplementary Figs. 2 and 3.

FLF-bearing crust. This generalized crustal type is 7.4–13.5-km thick along the Namibia lines. Beneath the earliest post-rift sediments (aptian–albian in age), the top basement is flat, sub-horizontal, and highly reflective. Beneath, are subhorizontal to gently seaward-dipping reflectors defining here the FLF facies that usually is much less reflective than SDRs (U1 in Fig. 4d; Supplementary Figs. 6 and 7). The geometric relationships between these reflectors and the edge of outer SDRs or inner SDRs may vary. In most of the studied sections, the reflectors onlap the seaward edge (U4 in Fig. 4d) of the outer- or else inner SDRs (Supplementary Fig. 6). In this latter case, FLF reflectors onlap onto the seaward-dipping lentical-shaped structures, if any (Supplementary Fig. 6a, b). The onlapping reflectors, albeit mostly parallel, may form a weakly defined wedge with dips decreasing seaward (Supplementary Fig. 6c, d). Some pinching out of the reflectors against the inclined SDR reflectors has been observed (Supplementary Fig. 6b). Many evidences of seaward-

prograding features are observed in the FLF facies (Supplementary Fig. 7).

No oblique reflections crosscut the FLF section. An overall transparent medium with sporadic chaotic seismic facies generally underlies the seaward-dipping reflectors located to the top (Supplementary Fig. 6). The FLF section overlays a highly reflective deeper basement (Fig. 4d, Supplementary Figs. 6 and 7) whose top is defined by a prominent planar reflector U2, which is dipping seaward (Fig. 4d). Reflector U2 may parallel the overlying weak reflector U1 located above (Fig. 4d; Supplementary Fig. 5b). This is the top of a very reflective medium associated with parallel and closely spaced reflectors dipping continentward (U3). Significantly, none of these reflectors prolongate in the FLF section (Fig. 4d and Supplementary Fig. 5b). This “deep basement” corresponds to the UCR reflections as described elsewhere^{14–16} (Fig. 5). The deep-basement roughness is apparently due to offsetting and tilting of U2 by numerous and

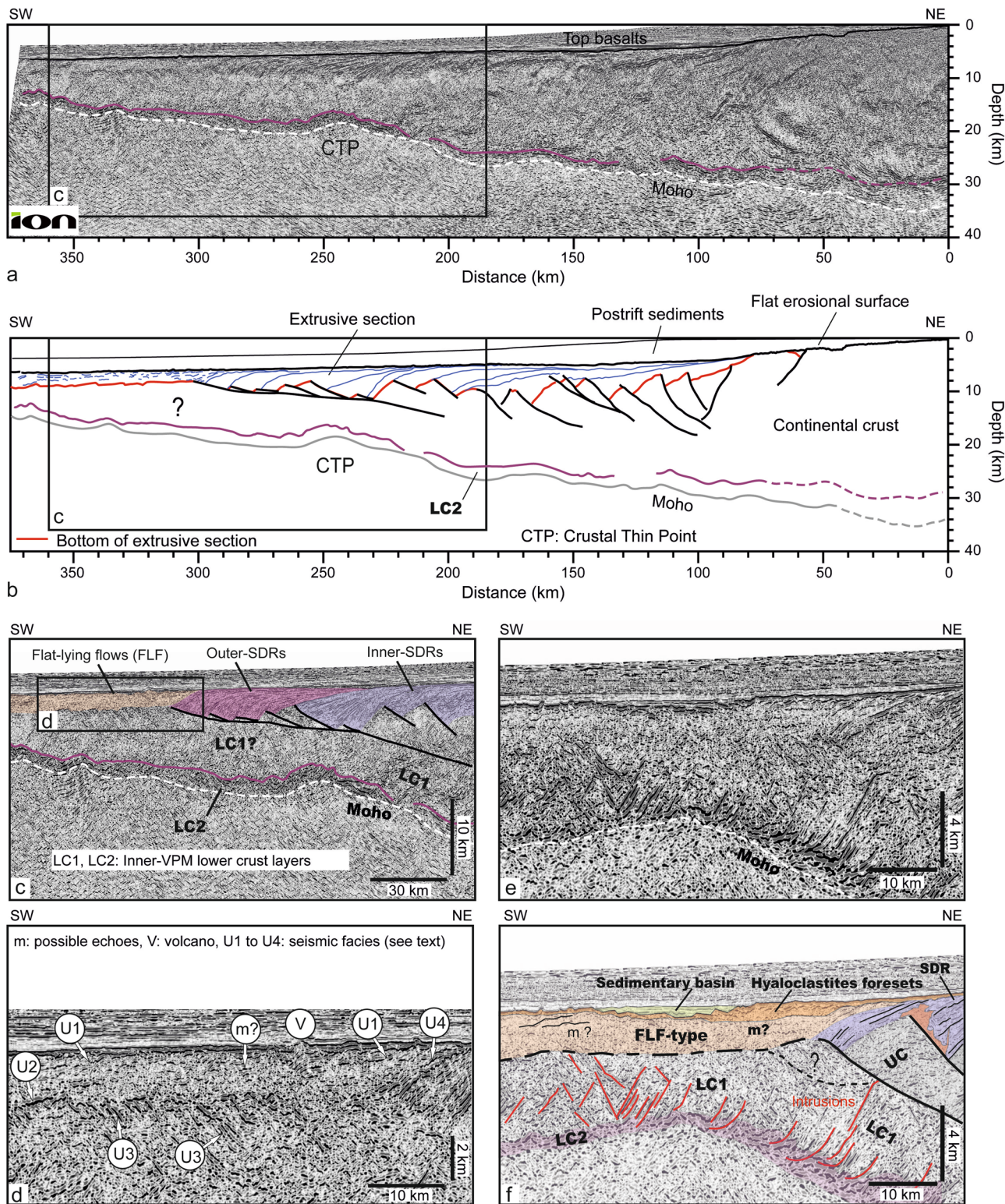


Fig. 4 Distal crustal types offshore Namibia. **a** S-Atlantic ION™ line II (Fig. 2); **b** line drawing. **c** and **d**. Close-ups of the outer edge of the margin (location in **a**, location of **d** in **c**; V volcano); **e**, **f** close-up of the outer edge of ION™ line VIII (Fig. 2). Some of the periodic reflections could be multiples (m) of the top-basement seismic horizon. An enlargement of Figs. 4d and 4e is given in Supplementary Fig. 5.

closely spaced (~6 ± 3 km) normal faults underlined by bright reflections, with vertical throws <800 m, all of them dipping continentward. These faults are parallel to the reflectors U3 (representing, probably, planar intrusions).

Beneath the UCR, the thick deep crust (corresponding to the distal crustal bulge) is characterized by a huge density in

high-energy planar reflectors that may dip either continentward (Fig. 4d) or both continentward and seaward, with, in this latter case, an X-shape pattern (Figs. 3 and 4e–f; Supplementary Fig. 4). This deep crust presents similar seismic facies with the lower crust from the adjacent necking zone (Supplementary Figs. 5a and 6c–d). Some continuity of the UCR facies beneath the

most distal SDR is observable in some lines (Supplementary Fig. 6c–d).

Crust type to seaward of the FLF crust. A crust with a constant thickness (6.0 ± 0.5 km), albeit with poorly defined Moho, is located to seaward of the distal crustal bulge (Figs. 2 and 3, Supplementary Fig. 4b). The top of the upper crust shows a marked roughness with abyssal hills 0.25 ± 0.15 km in amplitude, in significant contrast to the smoother top of the adjacent FLF crust. This rugosity is clearly due to continentward-tilted blocks bounded by clear discontinuities (normal faults) dipping seaward, spaced 3 ± 1 km, with throws not exceeding 0.6 ± 0.5 km, offsetting and tilting continentward top-basement reflectors. The underlying lower crust shows a few oblique reflectors.

Discussion

The interpretation of the FLF-type crust is a key point (Fig. 5A, B). The FLF-type crust has been interpreted as an unambiguous oceanic crust from TWT sections in the same area²² (Fig. 5B). The reflections at the top of the crust section were considered as layer 2A extrusives and the underlying more transparent medium to be dyke complexes (layer 2B) and isotropic gabbros. The more reflective deeper crust was considered to be a typical oceanic lower-crust gabbroic section (layer 3) (Fig. 5B). Our observations add more complexity (Fig. 5A). We outline, as others did^{15,16}, the seismic and geological importance of the so-called UCR reflections (U2 in Fig. 4d). Independently from the nature of the sub-UCR middle/lower crust (oceanic or not, see next section), we find evidence for the progressive seaward infilling (by probable volcano-sedimentary material) of a topographic depression bounded by a paleotopographic seaward-dipping monocline defined by the outer edge of the SDR-bearing crust. This slope may have formed during the progressive basin infilling. Indeed, the lens-shaped material to the top of the monocline (Supplementary Fig. 6a, b) has been interpreted either as tilted volcanoes or as large slumps along a seaward slope⁹. Both of these interpretations point to a top-UCR basin. We favor the former interpretation (i.e., volcanoes) due to the frequent stratified facies of the lens-shaped material (Supplementary Fig. 6b). The observed onlaps onto these tilted volcanoes imply that the observed seaward tilt of the most recent lavas (and overlying volcanoes) from the outermost-SDR wedge occurred during the progressive infilling of the basin. No horizontal variations in the Bouguer anomaly exists seaward the crustal thin point in the Namibian oceanic basin (Fig. 2). The FLF material thus probably filled in a basin 2 ± 1 -km thick, of mafic volcanic or volcano-sedimentary nature, whose subhorizontal basement would account for the strong UCR reflections (Fig. 5A). Seaward offlaps and pinching out of lavas/sediments against the convex paleotopography may suggest that the infilling material came from the inner VPM itself and not from a seaward location. This is also suggested by the occurrence in lines V–X (Fig. 2) of a late hyaloclastite subbasin, characterized by typical seaward-developing “foresets” passing, seaward, to sediments (Fig. 4e–f and Supplementary Fig. 5). These observations, as well as the smooth top surface of the FLF crust, also strongly suggest a subaerial paleoenvironment with lakes or shallow marine embayment just before deposition of the Aptian–Albian post-rift sediments. It should be noticed that some of the FLF facies that we observed, with seaward gently dipping reflections, have been elsewhere described as SDRs by others^{9,23}.

We hereafter question further if the outer-SDR- and FLF crust types, which are observed throughout the South-Atlantic margins, may be interpreted as oceanic in type (i.e., purely mafic and born from accretion at a ridge) (Fig. 5B).

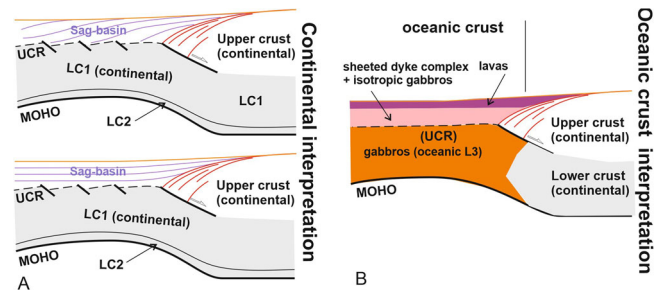


Fig. 5 Distinct interpretations for the FLF crust. **A** Continental interpretation. The top and left diagrams refer to distinct seismic facies observed in the basin. **B** Alternative oceanic-crust interpretation from seismic data from the same margins²².

Oceanic crusts usually have the following characteristics that are largely independent of the accretion rate^{24,25}: (1) an average thickness of about 6.15 ± 0.93 km²⁵; (2) when discernable, i.e., in less than 60% of seismic reflection studies, a flat-lying and most generally horizontal Moho with frequent sub-Moho reflections^{24,26,27}; (3) when discernable, a subhorizontal boundary between an upper crust ~ 1.5 -km thin with strong Vp gradient (“layer 2”; Vp ~ 4 – 6.5 km.s⁻¹) and a thicker lower crust with much lower velocity gradient (“layer 3”; Vp ~ 6.7 – 7.1 km.s⁻¹)^{25,28}; (4) strong and oblique reflections in the lower crust^{27,29–31}. At ultraslow to slow-spreading ridges (~ 10 – 40 mm.yr⁻¹ full rate), a high-amplitude subsediment roughness characterizes the top of the upper basaltic crust, associated with volcano-tectonic features and/or detachment faults exhuming the mantle³². Top-basement faults naturally tilt lavas “continentward”³³. It must however be noticed that ridgeward-dipping lavas have also been observed in conjunction with outward-dipping planar intrusions in intermediate- to fast-spreading ridges³⁴. Taken individually, none of the above characteristics can be considered as an accurate diagnostic tool for oceanic crust, however, a combination of them considerably increases the reliability.

Considering the criteria above, there is no doubt that the crust seaward to the distal crustal bulge is oceanic (Figs. 2 and 3). A spreading rate of ~ 50 mm.yr⁻¹ may be inferred from its roughness³⁵, in coherence with the 56 – 58 mm.yr⁻¹ early spreading rates as suggested from magnetic anomalies³⁶.

Considering our observations above concerning the outer-SDR and FLF crustal types, we encounter few or none of the characteristics listed above for oceanic crust, notably of slow-spreading type: (1) top-lava surfaces are smooth, (2) the lava (?) section appears not to be tectonized, (3) when not sub-horizontal, lavas tend to dip seaward (outer SDRs and FLF), (4) the Moho, clearly expressed, is neither horizontal nor flat, even at a small scale (~ 10 km), (5) crust thickness reaches twice the thickness of the “normal” oceanic crust nearby, (6) lower crust seismic velocities appear to overcome ($\sim +0.1$ km.s⁻¹ to $+0.4$ km.s⁻¹) those from the oceanic crust L3 layer, and (7) the thick high-velocity layer LC2 is unrecognized at oceanic crusts. The strong oblique reflections that are observed in the lower crust could be considered similar to those from the oceanic lower crust, but they are also observed in the Namibian VPM necking zone (e.g., Fig. 4f), which is usually considered as continental²². In addition, to account for our observations, considering that the top oceanic crust is the UCR would set a geometric issue to connect it to the top of the acknowledged oceanic crust seaward.

We thus alternatively propose that an exhumed middle–lower mafic continental crust could be located to seaward of the crustal thin point, whose top (UCR or U2 facies in Fig. 4d) would have been made brittle following the exhumation (Fig. 6a). A purely active and ductile exhumation mode, driven by lateral lithostatic

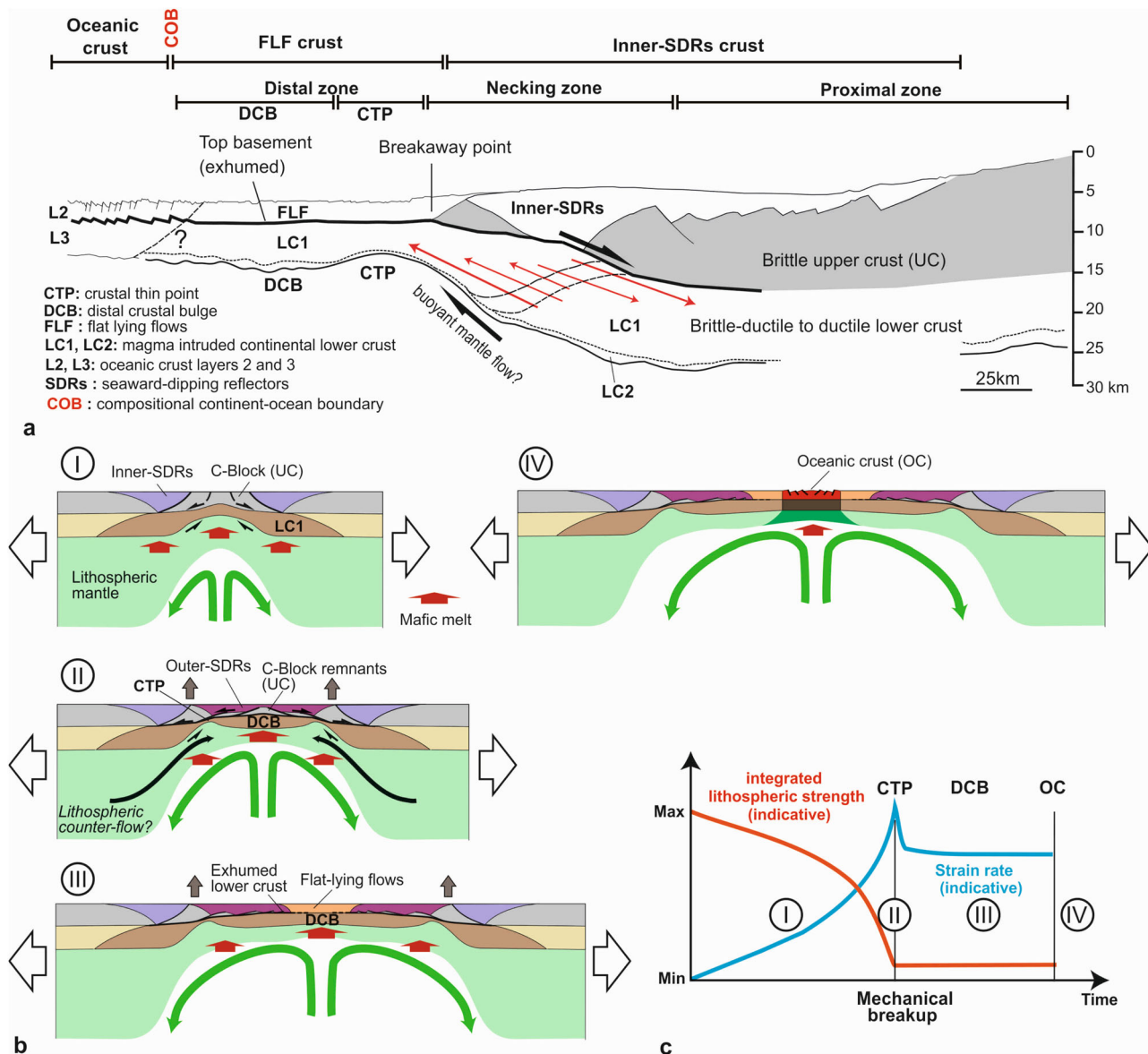


Fig. 6 Tectonic interpretation and breakup model. **a** Tectonic interpretation at crustal scale (drawn from IONTM line VI, Figs. 2, 3a); **b** suggested lithosphere evolution during breakup: crust necking (1), breaking up (2), and steady-state expanding in pure shear (3); **c** suggested strain rate and lithosphere integrated strength evolution with time. Numbers refer to (b).

pressure gradients, would involve an outward flow of a fully decoupled LC1 from the upper crust and from the postulated ultramafic LC2 (cumulates). This would imply (1) a long-term low viscosity of LC1 counteracting the hardening effects of mafic magma crystallization and (2) an opposite direction of shear at the bottom and top of LC1. Deformed reflectors (most probably a set of planar intrusions) rather suggest that LC1 as a whole is sheared top-to-continent¹² (Fig. 6a). A Couette-type flow of the entire lower crust is thus suggested (Fig. 6a). This overall continentward shear in the necking zone could be a consequence of a gravitational collapse detaching the upper crust from the passively exhumed highly mafic but still with continental remnants (LC1). A convective and buoyant mantle, explaining the permanent subaerial settings of lava emplacement, favored (or even provoked) this upper crustal detachment (Fig. 6a). The flat surface beneath outer SDRs (with possible allochthons) (Fig. 4c) would illustrate the detachment fault at its early stage. Outer SDRs would be dynamically bent over the detachment and thus be syntectonic features. FLF most certainly infilled the basin

during the progressive fault-controlled flexing of the external SDR wedges, as shown by the onlaps of FLF onto the tilted strato-volcanoes (previously horizontal). The progressively exhumed mafic LC1 experienced rapid embrittlement and some stretching during its exhumation, coeval with mantle melting.

Figure 6b summarizes the stages of the synmagmatic breaking up of the lithosphere and onset of the crust types as suggested in the South Atlantic. An initial continental block (C-Block in¹³), even of small size, is geometrically needed to create inner SDRs at paired margins^{3,13,23}. Due to high thermal fluxes, a significant part of the lithosphere strength lies within the mafic-intruded continental crust itself and especially in the ultramafic LC2 and in the dyke-intruded upper crust, whose large-wavelength monoclines (inner-SDR-related bending) attest to its rigidity. The bottleneck crustal thin point illustrates the sudden weakening of the continental lithosphere during this mechanical breakup, i.e., the sudden transition to a transient low-strength lithosphere due to detachment of the upper crust (Fig. 6c). A congruent transient peak in strain rate (Fig. 6c) is suggested by kinematic models in

the S Atlantic^{37,38}. Seaward of the crustal thin point, continental extension would be (1) steady state (Fig. 6c), (2) not isovolumic, tectonic thinning being overcompensated by magma addition, and (3) in pure shear, as suggested by the X-shape pattern of intrusions (Fig. 3). The 6.0 ± 0.5 -km thickness of the earliest oceanic crust is indicative of a normal potential temperature in the mantle¹ at the time of complete breakup of the lithosphere. Therefore, remnant continental material in the lower crusts of the outer SDRs and FLFs could range from 15 to 30% of the original thickness of the unstretched, unthinned lower continental crust along each line, assuming a constant rate and constant temperature of mantle melting beyond the crustal thinning point. The transition to oceanic crust is discrete (Fig. 6a). It is associated with the onset of an axial spreading/extensional system generating the type of mafic crust observed at slow-spreading ridges worldwide. This could be, strictly speaking, the limit of the compositional continental lithosphere.

Huismans and Beaumont³⁹ previously suggested that at some passive margins, exhumation of the continental lower crust could occur following a breaking up of the mantle lithosphere and the early setting of an oceanic-type convection. It is remarkable that their related II-A model reproduces a crustal thin point at the boundary between the rigid (still with mantle lithosphere) and weak lithosphere. These depth-dependent stretching models have been recently successfully applied to the formation of VPMS, explaining not only the extent of the continental realm but also the excess in synextension magmatism without significant excess in mantle temperature⁴⁰. Our interpretation would be the first to date to fully support depth-dependent extensional models at VPMS with continental lower-crust exhumation.

Conclusions

We discuss in this paper the extent of continental material seaward to the VPM necking zones, taking into example the Namibia volcanic passive margins. As far as we know, there are few equivalent of deep seismic reflection datasets comparable to the one available in the South Atlantic for the study of distal (and conjugate) VPMS^{8,41}. However, other observations elsewhere tend to support the unusual extent of continental material (crust and/or continental mantle) at VPMS, in the NE-Atlantic^{19,23}, Central Atlantic⁴² and Indian^{3,43} oceans. Notably, a continental interpretation is argued for the Cuvier Abyssal Plain SDR-bearing crust⁴⁴ offshore W Australia, which was previously considered as oceanic⁴⁵. Our observations may challenge previous oceanic crust interpretation of FLF- and/or outer-SDR crust types along some margins⁴⁶ where thin points and distal bulges may be observed. Considering that (1) more than 50% of margins worldwide are of volcanic-type and (2) the mafic extrusives of outer-SDR and FLF crusts generate perfect linear magnetic anomalies indistinguishable from those that are ridge-related^{17,18,44}, there is an obvious need to explore the distal edges of VPMS. At stake is our ability to determine the true extent of the oceanic lithosphere.

Methods

We mainly used long-offset prestack time-migrated seismic sections (PSTM), acquired by ION Geophysical in 2014. The multichannel seismic data were recorded for 18 s using a 10.2-km long, 804-channel streamer, a 50-m shot interval, and an air gun with a volume of 6,500 cu.in. The data acquired from ION Geophysical by TotalEnergies SE comprised 2 strike and 16 dip-prestack time-migrated sections, of which 3 sections (lines VIII, IX, and X in Fig. 2) were prestack depth-migrated (PSDM), involving ION-property applications and workflow processes. In this study, we specifically used the 10 dip sections lying south of the Walvis Ridge (Fig. 2). The depth conversion of the whole PSTM sections (lines I–X, Supplementary Figs. 2 and 3) was carried out using a 5-layer velocity model built by TotalEnergies SE. Four of these layers correspond to water and to a calibrated division of the post-rift sedimentary section, using industrial well data. Seismic velocities for the sedimentary layers were extracted from the ION PSTM data following Dix conversion and scaling. The basement section is considered as a

single layer whose velocities were largely inferred from velocities extracted from ION PSDM lines VIII, IX, and X (Fig. 2), which are close to the Kudu well⁴⁷. This bespoke model was compiled to fit both the Moho and the top-basalt horizons from the PSDM sections (lines VIII–X). Our model is compared with seismic refraction velocities inferred from available cross-cutting lines²¹ (Supplementary Figs. 2 and 3). We additionally show that the time to depth conversion does not change the bulk geometry of the main crustal features, notably the Moho topology (Supplementary Fig. 4). In addition to the ION dataset, we also used for the interpretation less-penetrative high-resolution PSTM lines from TGSTM (see Supplementary Figs. 6 and 7).

Data availability

Thanks to IONTM and TGSTM the seismic data supporting this study are available within the paper and the supplementary information file and can be used so to reproduce the findings. The raw data are private properties of IONTM and TGSTM which have to be contacted for any lending or acquisition.

Received: 9 June 2021; Accepted: 18 March 2022;

Published online: 19 April 2022

References

- White, R. et al. Magmatism at rifted continental margins. *Nature* **330**, 439–444 (1987).
- Eldholm, O. & Grue, K. North Atlantic volcanic margins: dimensions and production rates. *J. of Geophys. Res.* **99**, 2955–2968 (1994).
- Geoffroy, L., Guan, H., Gernigon, L., Foulger, G. R. & Werner, P. The extent of continental material in oceans: C-Blocks and the Laxmi Basin example. *Geophys. J. Int.* **222**, 1471–1479 (2020).
- Sutra, E., Manatschal, G., Mohn, G. & Unternehr, P. Quantification and restoration of extensional deformation along the Western Iberia and Newfoundland rifted margins: strain distribution along rifted margins. *Geochem. Geophys. Geosyst.* **14**, 2575–2597 (2013).
- Planke, S., Symonds, P. A., Alvestad, E. & Skogseid, J. Seismic volcanostratigraphy of large-volume basaltic extrusive complexes on rifted margins. *J. Geophys. Res.* **105**, 19335–19351 (2000).
- Agranier, A. et al. Volcanic record of continental thinning in Baffin Bay margins: Insights from Svartehuk Halvø Peninsula basalts, West Greenland. *Lithos* **334–335**, 117–140 (2019).
- Chauvet, F. et al. Eocene continental breakup in Baffin Bay. *Tectonophysics*. **757**, 170–186 (2019).
- Chauvet, F., Sapin, F., Geoffroy, L., Ringenbach, J. C. & Ferry, J. N. Conjugate volcanic passive margins in the austral segment of the South Atlantic—Architecture and development. *Earth Sci. Rev.* **212**, 103461 (2021).
- McDermott, C., Lonergan, L., Collier, J. S., McDermott, K. G. & Bellingham, P. Characterization of seaward-dipping reflectors along the South American Atlantic margin and implications for continental breakup. *Tectonics* **37**, 3303–3327 (2018).
- Buck, W. R. The role of magmatic loads and rift jumps in generating seaward dipping reflectors on volcanic rifted margins. *Earth Planet. Sci. Lett.* **466**, 62–69 (2017).
- Callot, J. P. & Geoffroy, L. Magma flow in the East Greenland dyke swarm inferred from study of anisotropy of magnetic susceptibility: Magmatic growth of volcanic margin. *Geophys. J. Int.* **159**, 816–830 (2004).
- Clerc, C., Jolivet, L. & Ringenbach, J. -C. Ductile extensional shear zones in the lower crust of a passive margin. *Earth Planet. Sci. Lett.* **431**, 1–7 (2017).
- Geoffroy, L., Burov, E. B. & Werner, P. Volcanic passive margins: another way to break up continents. *Sci. Rep.* **5**, 14828 (2015).
- Franke, D., Neben, S., Ladage, S., Schreckenberger, B. & Hinz, K. Margin segmentation and volcanotectonic architecture along the volcanic margin off Argentina/Uruguay, South Atlantic. *Mar. Geol.* **244**, 46–67 (2007).
- Soto, M. et al. The continental margin of Uruguay: crustal architecture and segmentation. *Mar. Petrol. Geol.* **28**, 1676–1689 (2011).
- Franke, D. et al. Birth of a volcanic margin off Argentina, South Atlantic. *Geochem. Geophys. Geosyst.* **11**, Q0AB04 (2010).
- Koopmann, H., Schreckenberger, B., Franke, D., Becker, K. & Schnabel, M. The late rifting phase and continental break-up of the southern South Atlantic: the mode and timing of volcanic rifting and formation of earliest oceanic crust. *Geol. Soc. London Spec. Pub.*, <https://doi.org/10.1144/SP420.2> (2014).
- Geoffroy, L., Gernigon, L. & Foulger, G. R. Linear magnetic anomalies and the limits of oceanic crust in oceans. In G. R., Foulger et al. (Eds.), In the Footsteps of Warren B. Hamilton: New Ideas in Earth Science. *Geol. Soc. Am. Spec. Pap.* **553**, 1–14 (2021).

19. Yuan, X., Korenaga, J., Holbrook, W. S. & Kelemen, P. B. Crustal structure of the Greenland-Iceland Ridge from joint refraction and reflection seismic tomography. *J. Geophys. Res.* **125**, e2020JB019847 (2020).
20. Senkans, A., Leroy, S., d'Acremont, E., Castilla, R. & Despinois, F. Polyphase rifting and break-up of the Central Mozambique margin. *Mar. Petrol. Geol.* **100**, 412–433 (2019).
21. Bauer, K. et al. Deep structure of the Namibia continental margin as derived from integrated geophysical studies. *J. Geophys. Res.* **105**, 25829–25853 (2000).
22. Norcliffe, J. R. et al. Laterally confined volcanic successions (LCVs); recording rift-jumps during the formation of magma-rich margins. *Earth Planet. Sci. Lett.* **504**, 53–63 (2018).
23. Quirk, D. G., Shakerley, A. & Howe, M. J. A mechanism for construction of volcanic rifted margins during continental breakup. *Geology* **42**, 1079–1082 (2014).
24. Mutter, J. C. & Carton, H. D. The Mohorovicic discontinuity in ocean basins: some observations from seismic data. *Tectonophysics* **609**, 314–330 (2013).
25. Christeson, G. L., Goff, J. A. & Reece, R. S. Synthesis of oceanic crustal structure from two-dimensional seismic profiles. *Rev. Geophys.* **57**, 504–529 (2019).
26. Nedimović, M. et al. Frozen magma lenses below the oceanic crust. *Nature* **436**, 1149–1152 (2005).
27. Kodaira, S. et al. Seismological evidence of mantle flow driving plate motions at a palaeo-spreading centre. *Nat. Geosci.* **7**, 371–375 (2014).
28. Detrick, R., Collins, J., Stephen, R. & Swift, S. In situ evidence for the nature of the seismic layer 2/3 boundary in oceanic crust. *Nature* **370**, 288–290 (1994).
29. White, R. S. et al. New seismic images of oceanic crustal structure. *Geology* **18**, 462–465 (1990).
30. Morris, E. et al. Seismic structure of oceanic crust in the western North Atlantic. *J. Geophys. Res.* **98**, 13879–13903 (1993).
31. Ding, W., Sun, Z., Dadd, K., Fang, Y. & Li, J. Structures within the oceanic crust of the central South China Sea basin and their implications for oceanic accretionary processes. *Earth Planet. Sci. Lett.* **488**, 115–125 (2018).
32. Buck, R., Lavier, L. & Poliakov, A. Modes of faulting at mid-ocean ridges. *Nature* **434**, 719–723 (2005).
33. Singh, S. et al. Discovery of a magma chamber and faults beneath a Mid-Atlantic Ridge hydrothermal field. *Nature* **442**, 1029–1032 (2006).
34. Karson, J. A. Geologic structure of the uppermost oceanic crust created at fast and intermediate-rate spreading centers. *Ann. Rev. Earth Planet. Sci.* **30**, 347–384 (2002).
35. Malinverno, A. Inverse square-root dependence of mid-ocean-ridge flank roughness on spreading rate. *Nature* **352**, 58–60 (1991).
36. Bird, D. E. & Hall, S. A. Early seafloor spreading in the South Atlantic: new evidence for M-series magnetochrons north of the Rio Grande Fracture Zone. *Geophys. J. Int.* **206**, 835–844 (2016).
37. Moulin, M., Aslanian, D. & Unternehr, P. A new starting point of the south and equatorial Atlantic Ocean. *Earth Sci. Rev.* **98**, 1–37 (2010).
38. Brune, S., Williams, S. E., Butterworth, N. P. & Müller, D. Abrupt plate accelerations shape rifted continental margins. *Nature* **536**, 201–204 (2016).
39. Huisman, R. & Beaumont, C. Depth-dependent extension, two-stage breakup and cratonic underplating at rifted margins. *Nature* **473**, 74–78 (2011).
40. Lu, G. & Huisman, R. S. Melt volume at Atlantic volcanic rifted margins controlled by depth-dependent extension and mantle temperature. *Nat. Commun.* **12**, 3894 (2021).
41. Sapin, F., Ringenbach, J.-C. & Clerc, C. Rifted margins classification and forcing parameters. *Sci. Rep.* **11**, 8199 (2021).
42. Bécel, A., Davis, J. K., Shuck, B. D., Van Avendonk, H. J. A. & Gibson, J. C. Evidence for a prolonged continental breakup resulting from slow extension rates at the eastern north American volcanic rifted margin. *J. Geophys. Res.* **125**, e2020JB020093 (2020).
43. Direen, N. G., Stagg, H. M. J., Symonds, P. A. & Colwell, J. B. Architecture of volcanic rifted margins: new insights from the Exmouth–Gascoyne margin, Western Australia. *Aust. J. Earth Sci.* **53**, 341–363 (2008).
44. Reeve, M. T. et al. Nature of the Cuvier Abyssal Plain crust, offshore NW Australia. *J. Geol. Soc.* **178**, jgs2020–jgs2172 (2021).
45. Rey, X., Planke, S., Symonds, P. & Faleide, J. I. Seismic volcanostratigraphy of the Gascoyne margin, Western Australia. *J. Volcanol. Geoth. Res.* **172**, 112–131 (2008).
46. Stagg, H. M. J. et al. Geology of the continental margin of Enderby and Mac. Robertson Lands, East Antarctica: Insights from a regional data set Marine. *Geophys. Res.* **25**, 183–219 (2008).
47. Wickens, H., de, V. & McLachlan, I. R. The stratigraphy and sedimentology of the reservoir interval of the Kudu 9A-2 and 9A-3 boreholes. *Com. Geol. Surv. Namibia* **6**, 9–23 (1990).
48. Hopper, J. R. et al. Structure of the SE Greenland margin from seismic reflection and refraction data: Implications for nascent spreading center subsidence and asymmetric crustal accretion during North Atlantic opening. *J. Geophys. Res.* **108**, 2269 (2003). B5.
49. Funck, T. et al. A review of the NE Atlantic conjugate margins based on seismic refraction data. In G., Péron-Pinvidic, et al. (Eds.), *The NE Atlantic Region: A Reappraisal of Crustal Structure, Tectonostratigraphy and Magmatic Evolution. Geol. Soc. London Spec. Pub.* **447**, 171–205 (2016).
50. Schuk, B. D., Van Avendonk, H. J. A. & Bécel, A. The role of mantle melts in the transition from rifting to seafloor spreading offshore eastern North America. *Earth Planet. Sci. Lett.* **525**, 115756 (2019).
51. Péron-Pinvidic, G. & Manatschal, G. The final rifting evolution at deep magma-poor passive margins from Iberia-Newfoundland: a new point of view. *Int. J. Earth Sci.* **98**, 1581–1597 (2008).
52. Mohn, G., Manatschal, G., Beltrando, M., Masini, E. & Kuszniir, N. Necking of continental crust in magma-poor rifted margins: evidence from the fossil Alpine Tethys margins. *Tectonics* **31**, TC1012 (2012).

Acknowledgements

This research was supported by the Total Energies SE-UBO GRI project “Volcanic Margins”. We warmly thank IONTM and TGSTM for granting permission to reproduce the seismic lines. We also acknowledge B. Shuck and Pr. S. Planke for their extensive and sound reviews. We are grateful to Klaus Bauer for providing the seismic refraction data from Namibia. A mention also for François Sapin and Yann Montico from Total Energies for stimulating discussion related to this study and to Glyn Orpwood for providing the English editing.

Author contributions

All authors analyzed and interpreted the seismic lines. L.G. wrote down the paper, made most figures and conceptualized the tectonic interpretation and geodynamic break-up model. F.C. produced Fig. 2 and the Supplementary data. JCR appraised the paper.

Competing interests

The authors declare no competing interests.

Additional information

Supplementary information The online version contains supplementary material available at <https://doi.org/10.1038/s43247-022-00420-x>.

Correspondence and requests for materials should be addressed to Laurent Geoffroy.

Peer-review information *Communications Earth & Environment* thanks Brandon Shuck and Sverre Planke for their contribution to the peer review of this work. Primary handling editors: João Duarte and Joe Aslin.

Reprints and permission information is available at <http://www.nature.com/reprints>

Publisher's note Springer Nature remains neutral with regard to jurisdictional claims in published maps and institutional affiliations.



Open Access This article is licensed under a Creative Commons Attribution 4.0 International License, which permits use, sharing, adaptation, distribution and reproduction in any medium or format, as long as you give appropriate credit to the original author(s) and the source, provide a link to the Creative Commons license, and indicate if changes were made. The images or other third party material in this article are included in the article's Creative Commons license, unless indicated otherwise in a credit line to the material. If material is not included in the article's Creative Commons license and your intended use is not permitted by statutory regulation or exceeds the permitted use, you will need to obtain permission directly from the copyright holder. To view a copy of this license, visit <http://creativecommons.org/licenses/by/4.0/>.

© The Author(s) 2022